NeuroImage: Clinical 28 (2020) 102373

Contents lists available at ScienceDirect

NeuroImage: Clinical

journal homepage: www.elsevier.com/locate/ynicl

More than meets the eye: Longitudinal visual system neurodevelopment in very preterm children and anophthalmia

Madelaine N.K. Gravelle[a,b,1], Marlee M. Vandewouw[a,b,1], Julia M. Young[a,b,e], Benjamin T. Dunkley[a,b,c,d], Manohar M. Shroff[a,c], Margot J. Taylor[a,b,c,e,*]

[a] Department of Diagnostic Imaging, Hospital for Sick Children, Toronto, Ontario, Canada
[b] Neurosciences & Mental Health Program, Hospital for Sick Children, Toronto, Ontario, Canada
[c] Department of Medical Imaging, University of Toronto, Toronto, Ontario, Canada
[d] School of Optometry and Vision Science, University of Waterloo, Waterloo, Ontario, Canada
[e] Department of Psychology, University of Toronto, Toronto, Ontario, Canada

ARTICLE INFO

Keywords:
Development
Diffusion tensor imaging
Monocular vision
Preterm
White matter

ABSTRACT

Anophthalmia, characterized by the absence of an eye(s), is a rare major birth defect with a relatively unexplored neuroanatomy. Longitudinal comparison of white matter development in an anophthalmic (AC) very preterm (VPT) child with both binocular VPT and full-term (FT) children provides unique insights into early neurodevelopment of the visual system. VPT-born neonates (< 32wks gestational age), including the infant with unilateral anophthalmia, underwent neuroimaging every two years from birth until 8 years. DTI images (N = 168) of the optic radiation (OR) and a control track, the posterior limb of the internal capsule (PLIC), were analysed. The diameter of the optic nerves (ON) were analysed using T1-weighted images. Significant group differences in FA and AD were found bilaterally in the OR and PLIC. This extends the literature on altered white matter development in VPT children, being the first longitudinal study showing stable group differences across the 4, 6 and 8 year timepoints. AC showed greater deficits in FA and AD bilaterally, but recovered towards VPT group means from 4 to 8 years-of-age. Complete lack of binocular input would be responsible for these early deficits; compensatory mechanisms may facilitate structural improvement over time. AC's ON exhibited significant atrophy ipsilateral to the anophthalmic eye. Functionally, AC displayed normal visual acuity and form perception, but naso-temporal bias in motion perception. Following these groups and AC longitudinally enabled novel understanding of the joint influence of monocular vision and VPT birth on neurodevelopment.

1. Introduction

Patterns of white matter development in very preterm (VPT) children are generally analogous to term-born populations, but with subtle differences in growth and compromised microstructure that influence long-term outcomes (Lebel et al., 2019; Young et al., 2017, Young et al., 2019). Early exposure to the ex-utero environment can have negative consequences for neural processes involved in white matter maturation including apoptosis, synaptic pruning, axonal retraction and synaptogenesis (Kostović and Jovanov-Milošević, 2006; Padilla et al., 2014). Cortical connectivity and myelination are particularly vulnerable to disruption (Pandit et al., 2013), as their development involves time and region-specific processes that take place early in life. Generally, the earlier a child is born, the greater the potential for decreases in cortical and subcortical connectivity (Lebel et al., 2019).

Children born VPT are at particular risk for white matter injury between 23 and 32 weeks gestational age (Back, 2017). White matter injury can impact vulnerable cell populations, such as the pre-oligodendrocytes, that are responsible for the pre-myelination of axons as well as the early subplate neurons (Ferriero & Miller, 2010). Over the course of development, downstream effects of white matter injury result in reduced myelination, cortical and subcortical development (Volpe, 2009). White matter lesions tend to be concentrated in the periventricular regions, followed by posterior and frontal regions (Guo

Abbreviations: VPT, very preterm; FT, full term; AC, anophthalmic child; GA, gestational age; MRI, magnetic resonance imaging; DTI, diffusion tensor imaging; FA, fractional anisotropy; MD, mean diffusivity; RD, radial diffusivity; AD, axial diffusivity; PLIC, posterior limb of the internal capsule; OR, optic radiation; ON, optic nerve; TBSS, tract based spatial statistics

* Corresponding author at: Diagnostic Imaging, Hospital for Sick Children, 555 University Ave., Toronto M5G 1X8, Ontario, Canada.
E-mail address: margot.taylor@sickkids.ca (M.J. Taylor).

[1] Contributed equally to this work.

https://doi.org/10.1016/j.nicl.2020.102373
Received 4 March 2020; Received in revised form 26 July 2020; Accepted 3 August 2020
Available online 06 August 2020

et al., 2017). As the visual system traverses the entire brain from anterior to posterior, higher incidences of impairment have been found from eye to cortex in children born VPT compared to full term neonates, independent of brain lesion and/or retinopathy of prematurity (ROP; Bassi et al., 2008; Pavaine et al., 2016). These impairments may result from a variety of factors, with previous research pointing to low birth weight and preterm birth *per se* as possible culprits (Fielder and Moseley, 2000; O'Connor et al., 2002; C. Kelly et al., 2014). O'Connor et al. (2002) also found increased incidence of reduced visual function and eye size. This last consequence could be particularly pertinent to a severe ocular malformation that has yet to be examined in the context of VPT birth: a rare congenital birth defect known as anophthalmia.

Characterized by the absence of one or both eyes, anophthalmia has an incidence rate of ~ 3–14 in 100,000 births, with no known sex or race differences (Källén et al., 1996). Other epidemiological risk factors include low birth weight/gestational age, multiple births and maternal age over 40 (Forrester and Merz, 2006; Verma and FitzPatrick, 2007). The neurobiological mechanisms of this condition are contested; some argue the condition results from abnormalities in optic vesicle and lens placode formation between the 22nd to 27th days of gestation in humans (Koole et al., 1990). More recent research by FitzPatrick and Heyningen (2005) suggests, however, the presence of optic nerves, chiasm and/or tracts in patients with anophthalmia are evidence for the regression of a partially developed eye, as opposed to aplasia of the optic vesicle(s). Extraocular muscle insertion into what is possibly an aborted eye observed in anophthalmic sockets further supports this theory. Regardless of causation, there is complete lack of light or endogenous firing input from the missing eye(s) to the visual system, which would impact neural organization patterns in the brain (Verma and FitzPatrick, 2007; Shiell, 2014).

To date, research on individuals with only one eye has focused on the consequences of enucleation (removal of the eye(s)), usually due to retinoblastoma, where the eye is removed typically in the first three years of life (Budny and Grochowski, 2018; Gargallo et al., 2018). These studies have shown early life enucleation to impact patterns of myelination and reduce axon density in the visual pathways in childhood (Dunkley et al., 2019), which are sustained long-term (Kelly et al., 2015; Wong et al., 2018). Overall degeneration of the anterior ipsilateral visual system is apparent, but the aspects contralateral to the enucleated eye are more severely impacted by the loss of binocular vision (K. Kelly et al., 2014). Functionally, although enucleates show deficits in form perception and motion processing, plasticity, neural recruitment of resources to the remaining eye, and years of monocular practice enable those with monocular vision to have relatively normal vision (González et al., 2008).

Few studies have examined enucleation in children determining the impact on brain development (Barb et al., 2011), and even less attention has been given to the neurodevelopment of those born without one or both eyes. Furthermore, an extensive comparison of VPT and full-term (FT) children holds potential for enhancing our understanding of the ontogenetic consequences of VPT birth. Given the nature of anophthalmia and a unique longitudinal dataset, this study used diffusion tensor imaging (DTI) to provide novel insights into the joint neuroanatomical impacts of VPT birth and exclusively monocular vision in a VPT-born unilaterally anophthalmic child (AC) over the first eight years of life, contextualized by VPT and FT peers and by AC's functional outcome. In AC's case, absence of the right eye (and therefore binocular visual input) was expected to catalyze asymmetrical development of the visual system, with left-lateralized reductions in white matter development due to the degree of decussation of optic nerve fibres in the chiasm (Remington, 2012).

2. Materials and methods

2.1. Participants

One hundred and two VPT neonates (born < 32wks GA), including one anophthalmic child (AC), were recruited from the neonatal intensive care unit at the Hospital for Sick Children in Toronto as part of a longitudinal study. Exclusion criteria for recruitment included known major congenital or chromosomal abnormalities. The participants underwent DTI scanning within two weeks of birth, and were invited back for follow-up scanning at term-equivalent age, and at two, four, six and eight years of age. Sixty-six FT control participants were recruited at four, six or eight years of age and underwent DTI scanning, and were invited back for follow-up scanning at the remaining time points. The absence of any learning, language, neurological or developmental disabilities was a requirement for the recruitment of the FT children. Parents gave informed written consent, and children aged four years and older gave informed verbal assent, according to the Declaration of Helsinki. The research ethics board at the Hospital for Sick Children approved the study protocol.

2.2. MRI acquisition

At birth and term-equivalent age, the VPT neonates were scanned swaddled and naturally sleeping. A nurse administered a mild sedative (chloral-hydrate) to the VPT children at the two-year point to assist with obtaining sufficient quality data. At four, six and eight years of age, data for both the VPT and FT children were acquired while watching a movie or under natural sleep. The DTI acquisition protocols at each time point can be found in Table 1. Sagittally-acquired T1-weighted imaging data were also collected on AC at the two-, four-, six- and eight-year time points; corresponding acquisition protocols can be found in Supplemental Table 1.

Table 1
The DTI acquisition protocol at each time point.

DTI acquisition details	Preterm	Term	2 Year	4 Year	6 Year	8 Year
MRI scanner	1.5 T GE Signa Excite HD	1.5 T GE Signa Excite HD	1.5 T GE Signa Excite HD	3 T Siemens MAGNETOM Trio	3 T Siemens MAGNETOM Trio	3 T Siemens MAGNETOM PrismaFIT
Coil	Neonatal head	Neonatal head	12 channel head	12 channel head	12 channel head	12 channel head and neck
Sequence	SE-EPI	SE-EPI	SE-EPI	SE-EPI	SE-EPI	SE-EPI
b-value (s/mm^2)	700	700	700	1000	1000	1000
# directions	15	15	15	60	60	30
# B0 volumes	3	3	3	8	8	6
TR/TE (s)	15/0.085	15/0.085	15/0.085	8.8/0.087	8.8/0.087	3.9/0.073
FOV (mm)	205 × 205	224 × 224	368 × 368	244 × 244	244 × 244	244 × 244
Resolution (mm)	0.8 × 0.8	0.88 × 0.88	1.44 × 1.44	2 × 2	2 × 2	2 × 2
# slices	49	47	60	70	70	70
Slice thickness (mm)	1.6	1.6	2.3	2	2	2
Collected (VPT:FT)	102:0	57:0	20:0	33:28	30:36	30:41

SE-EPI: spin-echo echo-planar imaging; TR: repetition time; TE: echo time; FOV: field of view; VPT: very preterm; FT: full-term

2.3. Optic nerve diameters

To examine the anterior aspect of AC's visual system at the two-, six- and eight-year time points, the T1-weighted images were reoriented using RadiAnt DICOM Viewer (RadiAnt, 2019) to ensure the optic nerves (ONs) were observed in the same plane across scans. At each time point, bilateral ON diameter measurements were obtained 0 mm, 3 mm and 7 mm posterior to the lamina cribrosa in the adjusted axial and sagittal views. AC's T1-w images from the preterm, term-equivalent and 4-year timepoints had poorer image quality, making it difficult to accurately measure the optic nerve diameters, and thus were not included.

2.4. DTI processing

The DTI data were corrected for eddy current distortions and subject movements by aligning each volume to a reference B_0 volume and correspondingly realigning the *b*-vectors using FMRIB's Linear Image Registration Tool (Jenkinson and Smith, 2001; Jenkinson et al., 2002) and custom scripts. Each dataset was visually inspected for volumes corrupted by motion, which were excluded. Datasets with the number of corrupted volumes exceeding a threshold were excluded from the analysis: for the 15-direction datasets (obtained at birth, term-equivalent, and two years of age), up to five volumes were excluded; for the 60-direction datasets (obtained at four and six years of age), up to 30 volumes were excluded; for the 30-direction dataset (obtained at eight years of age), up to 10 volumes were excluded. The number of collected versus final datasets at each time point can be found in Table 1.

The diffusion tensor was estimated using the Robust Estimation of Tensors by Outlier Rejection (RESTORE) method (Chang et al., 2005) and used to estimate fractional anisotropy (FA), radial diffusivity (RD), axial diffusivity (AD) and mean diffusivity (MD) images for each dataset. For each of the birth, term and two-year-old time points, *MICe-build-model* (Lerch et al., 2010) was used to non-linearly co-register the FA images, creating an FA template. For each of the four-, six- and eight-year-old time points, tract-based spatial statistics (TBSS; Rueckert, 1999; Smith, 2002; Smith et al., 2004; Smith et al., 2006; Andersson et al., 2007a,b) were used to align the FA images to the MNI152 standard space template via the most representative image, and the mean of all the aligned FA images was used as an FA template. For each time-point, the generated transformations were also applied to the RD, AD and MD images, aligning them into template space. Using TBSS, the FA templates at each time point were thinned and thresholded at $FA > 0.2$ to create an FA skeleton, representing a mask of the centres of all white matter tracts. Each subject's data (FA/MD/AD/RD) in template space were then projected onto this skeleton.

The bilateral optic radiations (ORs) and posterior limbs of the internal capsule (PLICs) were manually delineated from each timepoint's FA template. The PLIC was chosen as a control tract, and since no hemispheric differences were hypothesized, the PLIC masks were combined across hemispheres. The identified tracts were masked with the corresponding FA skeleton, resulting in masks representing the centre of the left OR, right OR, and bilateral PLICs (Fig. 1). Mean FA, RD, AD and MD values within each tract were extracted.

To ensure that significant effects in the subsequent statistical analyses using the DTI metrics were not being driven by differences in acquisition protocols across the time points (see Table 1), a batch-effect correction tool called ComBat (Johnson et al., 2007) was also used on the FA, AD, RD and MD maps. ComBat was introduced as a non-parametric empirical Bayes framework for adjusting data for batch effects, and has recently been reformatted and validated for use on maps of DTI metrics (Fortin et al., 2017). Time points with the same acquisition scanner, TR, TE, b-value and number of directions were interpreted as a batch (thus three batches: the GA, term and two-year time points, the four- and six-year time points, and the eight-year time point), and the ComBat algorithm was run with age, group (VPT or FT) and sex as covariates.

2.5. Statistics

At the four-, six- and eight-year old time points, differences in age between the VPT and FT children were tested using Mann-Whitney U tests (chosen due to the non-normality of the age distribution), while Chi-squared tests were used to test for differences in sex ratio.

In each tract (left OR, right OR and bilateral PLIC), differences in FA, RD, AD and MD between the VPT and FT children across age (the four-, six- and eight-year time points) were investigated using linear mixed effects models. In the models, each participant was modeled as a random effect and age and sex were used as nuisance covariates. Within each tract, resulting *p*-values were corrected for multiple comparisons across the four DTI metrics using Bonferroni correction, with significance held at $p_{corr} < 0.05$. To establish significant changes with age in each tract for each DTI metric, linear mixed effects models were used across all time points, controlling for group (VPT or FT) and sex, with significance held at $p_{corr} < 0.05$. The analyses of the DTI metrics were repeated for the ComBat-harmonized data.

2.6. Assessment of visual function

At 8 years of age, AC completed a 2-alternate forced choice (2AFC) 2-down 1-up interleaved staircase (at least 2 sessions), random-dot-kinematogram (RDK) global motion procedure. In this test, participants fixate a central crosshair, around which 100 dots are presented within a 5-degree aperture. Dot speed was set at 6 deg/s, with a dot density of 1.27 dot/deg^2. Stimuli were generated using Psychkinematix software (Beaudot, 2008). The standard Freiburg acuity and contrast sensitivity tests (Bach, 2007) were also completed with AC.

2.7. Data availability statement

The data that support the findings of this study are available from the corresponding author upon reasonable request.

3. Results

3.1. Participant characteristics

The demographics of the participants included in the analyses are summarized in Table 2. AC is male and was born at a GA of 30.9 weeks. The FT children were older than the VPT at the four-year-old time point ($U = 32.44, p = 1.23 \times 10^{-8}$), but there were no significant differences in age at the six- ($U = 1.13, p = 0.29$) or eight- ($U = 1.51, p = 0.22$) year time points. There were no differences in sex ratio between the VPT and FT children at the four- ($\chi^2 = 58.00, p = 0.23$), six- ($\chi^2 = 60.32, p = 0.39$) or eight- ($\chi^2 = 67.94, p = 0.34$) year time points.

3.2. Visual function and optic nerve development

Visual function of AC was within normal range for acuity and contrast sensitivity, but he showed an asymmetry in motion perception (reduced in nasal-moving RDK), with a ratio of only 0.28 (ideally around 1 in the general population), which is consistent with studies on enucleated patients (Kelly et al., 2013). AC's ON diameter ipsilateral to the missing eye exhibited significant anterograde degeneration, while the diameter of the contralateral ON grew across all time points (Fig. 2).

3.3. Developmental trends in white matter

The mean FA, RD, AD and MD in the bilateral PLIC, left OR and right OR in the VPT group, FT group, and AC can be seen in Fig. 3, and the data are tabulated in Supplemental Tables 2-4. The VPT cohort

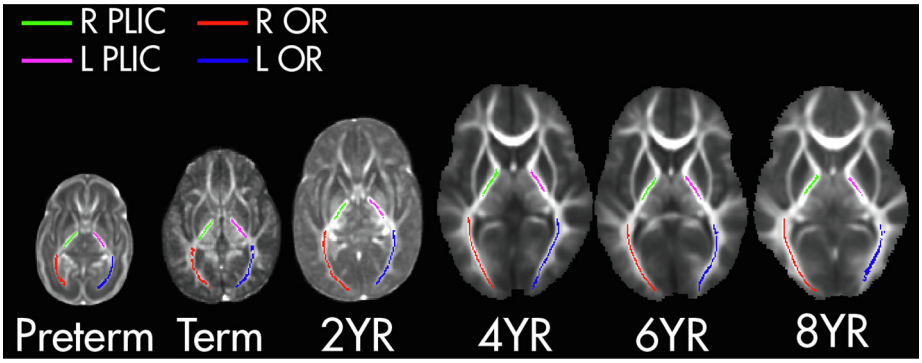

Fig. 1. Axial slices of average FA templates with overlaid white matter skeletons and ROI masks (green: right PLIC, pink: left PLIC, red: right OR, blue: left OR) at each sampled time point. (For interpretation of the references to colour in this figure legend, the reader is referred to the web version of this article.)

showed reduced FA and AD bilaterally in the OR compared to the FT, as well as left-lateralized increases in RD (Table 3). Significant reductions in AD in the VPT compared to FT children were also found in the PLIC. AC generally followed the developmental trends observed in his VPT peers, but presented with greater OR reductions in FA and AD (Fig. 3). Peak disparity between AC and the other cohorts was reached at 6 years of age, however recovery towards group means was seen in AC between 6 and 8 years of age across both measures. Interestingly, FA in AC's PLIC trended within the higher range of both groups across all time points. Across both groups, age was significantly positively correlated with FA in the three tracts, while age was negatively correlated with AD, RD and MD (Supplemental Table 5, Fig. 3). Corresponding results for the ComBat-harmonized data are presented in Supplemental Fig. 1 and Supplemental Tables 6–7.

4. Discussion

Previous literature lacks an in-depth neurobiological analysis of those with unilateral anophthalmia, as most animal and human studies focus on binocular presentation of the condition (Halilbasic et al., 2018). To our knowledge, we are the first to investigate the neuroanatomical development of an anophthalmic child within a longitudinal timeframe. We are also the first to complement this case study with comparative data to provide novel understanding of how both exclusively monocular vision and VPT birth influence the maturation of the visual system from preterm birth through to mid-childhood. Broadly, our findings suggest that white matter development is compromised by preterm birth, which is consistent with previous DTI studies of preterm populations (Bassi et al., 2008; Padilla et al., 2014; Pavaine et al., 2016; Young et al., 2017). Bilaterally reduced FA and AD, along with left-laterally increased RD in the OR, reflect disruptions in early life maturation processes. The anophthalmic child (AC) exhibited further deficits across the same measures in the OR, but interestingly, showed enhanced FA bilaterally in the PLIC across all time points. When coupled with reductions in RD, as well as recovery towards group means seen in the OR, these findings suggest that there are compensatory mechanisms facilitating improvement in microstructural white matter development over time in AC. Regarding the anterior visual system of AC, lack of visual input due to the missing right eye would be responsible for atrophy of the ipsilateral optic nerve (ON), in contrast to the growth exhibited in the contralateral ON over time. It is important to note that all descriptions of the findings regarding AC are qualitative in nature, as no statistical analyses could be conducted to quantitatively assess the differences between AC and the two cohorts.

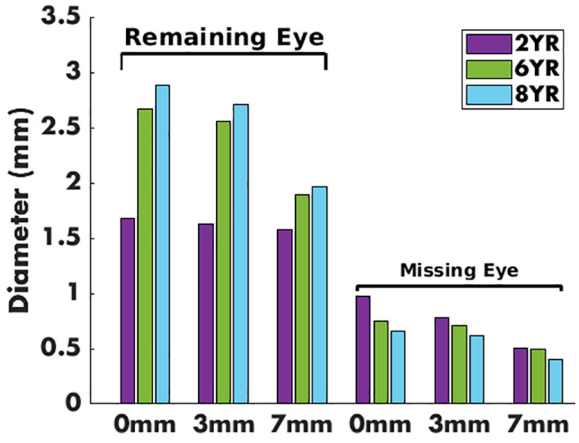

Fig. 2. Bilateral optic nerve diameter measurements 0, 3 and 7 mm posterior to the lamina cribrosa for the anophthalmic child at 2 (purple), 6 (green) and 8 (blue) years of age. (For interpretation of the references to colour in this figure legend, the reader is referred to the web version of this article.)

Overall, the VPT cohort, along with AC, had patterns of FA increases and MD, RD and AD decreases across time points; a ubiquitous pattern related to white matter development during childhood and adolescence (Suzuki et al., 2003; Alexander et al., 2007; Lebel et al., 2019). The rate

Table 2
Participant demographics.

Details		Preterm	Term	2 Year	4 Year	6 Year	8 Year
Final sample (Collected)	VPT	75 (102)	39 (57)	18 (20)	31 (33)	30 (30)	30 (30)
	FT	0 (0)	0 (0)	0 (0)	28 (28)	34 (36)	41 (41)
Median adjusted age(years; ± std.)	VPT	0.64 ± 0.07	0.81 ± 0.04	2.86 ± 0.11	4.68 ± 0.18	7.04 ± 0.34	9.11 ± 0.56
	FT	–	–	–	5.32 ± 0.31	7.29 ± 0.60	9.29 ± 0.47
Sex (M:F)	VPT	41:34	17:22	11:7	16:15	17:13	16:14
	FT	–	–	–	13:15	16:18	21:20
Mean GA(weeks; ± std.)	VPT	28.9 ± 1.7	29.0 ± 1.3	28.8 ± 1.8	28.5 ± 1.7	28.9 ± 1.4	28.8 ± 1.2
	FT	–	–	–	39.6 ± 1.0	39.2 ± 1.3	39.3 ± 1.3
GA-adjusted age (years)	AC	0.75	0.86	2.90	4.62	6.87	8.71

N: Number of participants with usable DTI data; VPT: very preterm; FT: full-term; M: male; F: female; GA: gestational age; AC: anophthalmic child

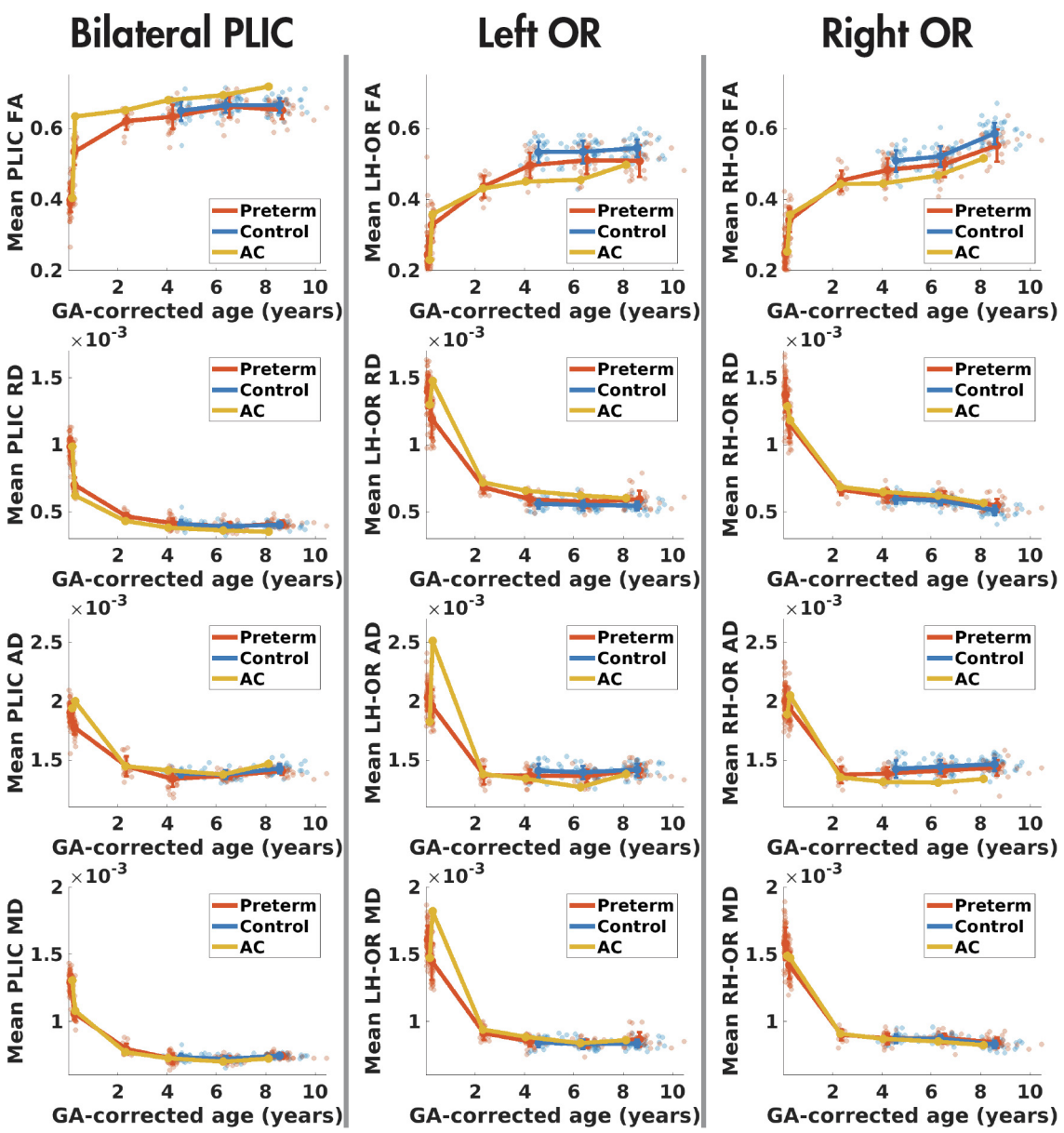

Fig. 3. Mean measures of FA, MD, RD and AD in the bilateral PLIC, left OR, and right OR for the VPT cohort (orange), FT cohort (blue) and AC (yellow) across the six time points. (For interpretation of the references to colour in this figure legend, the reader is referred to the web version of this article.)

Table 3
Group differences in white matter development in the bilateral PLIC, left OR and right OR between the VPT and FT groups across age. Significant p_{corr} values (< 0.05) are bolded.

ROI	Metric	Significant effect	Parameter estimate(± std. error)	*t*-statistic	p_{corr}
PLIC	FA	–	$6.22 \times 10^{-3} \pm 4.95 \times 10^{-3}$	1.26	0.84
	RD	–	$4.65 \times 10^{-7} \pm 5.17 \times 10^{-6}$	0.09	1.00
	AD	FT > VPT	$2.03 \times 10^{-5} \pm 0.73 \times 10^{-5}$	2.79	**0.02**
	MD	–	$5.99 \times 10^{-6} \pm 4.20 \times 10^{-6}$	1.42	0.64
L OR	FA	FT > VPT	$2.84 \times 10^{-2} \pm 0.67 \times 10^{-2}$	4.23	$\mathbf{1.43 \times 10^{-4}}$
	RD	FT < VPT	$2.97 \times 10^{-5} \pm 0.82 \times 10^{-5}$	3.61	$\mathbf{1.56 \times 10^{-3}}$
	AD	FT > VPT	$2.58 \times 10^{-5} \pm 0.98 \times 10^{-5}$	2.63	**0.04**
	MD	–	$1.03 \times 10^{-5} \pm 0.68 \times 10^{-5}$	1.52	0.52
R OR	FA	FT > VPT	$2.14 \times 10^{-2} \pm 0.68 \times 10^{-2}$	3.17	**0.01**
	RD	–	$1.84 \times 10^{-5} \pm 0.76 \times 10^{-5}$	2.42	0.07
	AD	FT > VPT	$3.44 \times 10^{-5} \pm 1.16 \times 10^{-5}$	2.96	**0.01**
	MD	–	$8.29 \times 10^{-6} \pm 6.31 \times 10^{-6}$	0.13	1.00

PLIC: posterior limb of the internal capsule; OR: optic radiation; FA: fractional anisotropy; RD: radial diffusivity; AD: axial diffusivity; MD: mean diffusivity; FT: full-term; VPT: very preterm

of these widespread developmental changes in white matter are most rapid during the first few years of life (1%/week during early infancy and ~ 5–10%/year in early childhood), which explains the near-exponential increase in FA and decrease in MD/RD/AD between birth and 2 years of age in our VPT cohort and AC (McGraw et al., 2002; Hermoye et al., 2006; Oishi et al., 2013). Accelerated rate of development between preterm birth and term-equivalent age indicates that time spent in-utero is incredibly important for proper maturation of white matter in early life (Qiu et al., 2015). Even within the first 2 years of life, pervasive increases in axon diameter and myelination (Yakovlev and Lecours, 1967; Lecours, 1989) are echoed in DTI metrics (Dubois et al., 2014; Huang and Vasung, 2014; Lebel et al., 2019). Our findings of left-lateralized increased RD and decreased AD (in the VPT OR and PLIC, respectively, compared to FT controls) support other reports of hemispheric asymmetry of age-related changes (Dubois et al., 2008; Kasprian et al., 2008; Lebel et al., 2012; Akazawa et al., 2016).

AC exhibited relatively high FA values in the PLIC, yet within the range of the VPT cohort. Lower RD values were also seen within the PLIC, suggesting that the higher FA was likely due to myelination. The PLIC encompasses a heterogeneous group of sensorimotor white matter tracts; the majority of the tract contains motor fibres from the cortical spinal tract, while the remaining portion contains fibres involved in sensory, vision and hearing (Sullivan et al., 2010). It is likely that the trajectory of AC's PLIC is primarily due to the development of motor or other sensory inputs. It is also interesting to note that there was little difference between the VPT group and the FT controls between 4 and 8 years of age, indicating similar development of the PLIC between the two groups into mid-childhood.

Extending the studies in the literature of VPT children tested at various ages and usually cross-sectionally, these current data demonstrate that the VTP-FT group differences remain stable across the four, six and eight-year time points. This reinforces the model that it is the fact of being born early in the third trimester, a period critical for the foundation of normal white matter maturation (Kostović and Jovanov-Milošević, 2006), that underlies these long-lasting differences, not a maturational lag. Although white matter development appears to asymptote at around five years of age, evident in both the FT and VPT cohorts of this study, considerable data show neurodevelopment continues past this stage, albeit at a slower rate (0.5%/year in late childhood and adolescence; Lebel et al., 2019). The VPT cohort followed the general developmental trajectory seen in those born FT, but their FA and AD measures trended significantly below those of the FT cohort in both ORs; likely reflecting disrupted myelination and/or neural organization (Beaulieu and Allen, 1994; Harsan et al., 2006; Tyszka et al., 2006). Myelin is known to modulate the amount and direction of anisotropy within a given fibre bundle (Beaulieu and Allen, 1994), indicating that reduced axon myelination may be partially responsible for the FA differences seen in this cohort.

Additionally, early ex-utero environmental exposure may be impacting axon membrane permeability, thereby reducing the density of axonal packing and/or the coherence of axon orientations (Beaulieu, 2002; Song et al., 2005; Sun et al., 2006), all of which would be evident in the AD measures of the white matter tracts. Importantly, despite there being no evidence of catch-up in the VPT children in the DTI metrics, the differences were not worsening either. This is critical, as the cognitive and behavioural difficulties often worsen over school age (e.g., Aarnoudse-Moens et al., 2012). This first report of longitudinal DTI data from birth through toddlerhood and into mid-childhood in VPT children, compared to FT controls, would suggest greater interventional support for these children, as the structural changes effected very early in life are not worsening, thus the functions that they underpin could be reinforced.

Although AC followed the developmental trend of the VPT cohort, his left OR displayed emerging FA and AD differences at 4 years of age. This change was in contrast with the trajectory of the right OR, which displayed a developmental trajectory close to the other groups. The mechanisms behind AC's asymmetrical deficits are a complex impact of his ocular malformation. When considered within the context of the visual pathway, decussated visual input from the contralateral eye represents more than 50% of input received by an OR (Petros et al., 2008). Neither OR is receiving a complete picture: the right OR is missing the small amount of ipsilateral visual stimulation, but the anatomical consequences of this absence are not as drastic as those resulting from missing contralateral input to AC's left OR. The resulting asymmetries in the ORs are greater than those seen in the VPT cohort, indicating that preterm birth and a lack of binocular input are both influencing the development of AC's visual system. Recovery toward group means in later time points, however, suggests the presence of compensatory mechanisms, such as neural plasticity (Wong et al., 2018), facilitating improvements in structural development over time. This is in contrast to the lack of compensatory developmental catch-up on the deficits attributable to being born VPT.

Similar patterns of compromised white matter microstructure in AC are also seen in the OR of enucleates. Previous studies have found that removal of an eye in early life is a causal factor in the observed lateralized AD and FA reductions contralateral to the enucleated eye (Wong et al., 2018; Dunkley et al., 2019). Physiologically, due to the correspondingly greater number of crossed than uncrossed ganglion cell axons in the visual system, the OR contralateral to the enucleated eye has larger declines in innervation (K. Kelly et al., 2014; Dunkley et al., 2019). Studies of anophthalmic neuroanatomy also revealed a symmetrical distribution of the remaining eye's optic axons through the chiasmatic pathways (Neveu et al., 2006), which, when coupled with the results of our OR analysis, show the hemispheric projections from AC's remaining eye also follow normal patterns of decussation.

Investigation of AC's anterior visual system over time showed significant decreases in ON diameter ipsilateral to the missing eye, along with growth of the contralateral ON of the remaining eye. These asymmetries were expected, as the lack of the eye and the corresponding visual stimulation would be responsible for the observed atrophy. A previous study on early monocular enucleates in adulthood has seen similar asymmetries in the ONs; K. Kelly et al. (2014) found diameter measurements of early monocular enucleates to be larger than those seen in our AC; however, their report of a relationship between age at enucleation and smaller ON morphology, along with normative paediatric data from Al-Haddad et al. (2018), provide context for the greater decreases in ON width in AC's childhood. These differences highlight the distinction between the developmental impacts of early eye removal, as opposed to a lack of development in the first place.

Functionally, AC performed within normal range across most visual assessment measures (acuity and contrast sensitivity), only showing deficits in temporalward motion perception. Behavioural data from Reed et al. (1991) found this same nasalward motion bias in enucleates. The physiological explanations suggest that crossed nasal fibres may be recruiting geniculate cells associated with the enucleated eye, which results in the cortical space having higher levels of innervation from the remaining eye (Rakic, 1981; González et al., 2008; K. Kelly et al., 2014). A lifetime's worth of monocular practice and no binocular inhibitory interactions would also contribute to these anatomical changes and their consequences for symmetrical motion perception (González et al., 2008). AC from our study presents with an even greater naso-temporal asymmetry than the sampled enucleates, suggesting that this biological phenomenon is more pronounced in those with anophthalmia.

4.1. Limitations

Possible limitations of this study include changes in diffusion protocol between time points; the number of directions acquired using a 3 T scanner from four-years onwards was greater than that obtained from GA to two years of age on a 1.5 T scanner (60 direction vs. 15 direction). Therefore, the data collected during the later timepoints may be more reliable. Also, retention of subjects past the initial

recruitment scan proved challenging, especially at the two-year time point when there was a need for sedation of participants to obtain clean scans during image acquisition.

4.2. Conclusion

Our longitudinal examination of children born VPT, FT and an anophthalmic child provided a uniquely contextualized understanding of the influence VPT birth and exclusively monocular vision have on both structural and functional neurodevelopmental outcomes. The observed trends in DTI metrics reflected the underlying compromised white matter microstructure in the visual systems of both binocular and the anophthalmic VPT-born children. Additionally, the asymmetrical development in the anterior aspect of the anophthalmic child's visual system would have been an influential factor in the asymmetries of white matter maturation in his optic radiations. By extending the work of Young et al. (2017), as well as including normative subjects and an anophthalmic preterm child, we had the exceptional opportunity to offer seminal knowledge of plausible determinants of white matter maturation in those born preterm and/or without an eye.

Declaration of Competing Interest

The authors declare that they have no known competing financial interests or personal relationships that could have appeared to influence the work reported in this paper.

Acknowledgements

We would like to thank all of the families who participated in our study, as well as Dr. Benjamin A.E. Hunt and Justine Ziolkowski for their valued support, and our wonderful MRI technologists – Tammy Rayner and Ruth Weiss - without whom this study could not have been completed. This work was supported by the Canadian Institutes of Health Research (MOP-84399 and MOP-137115).

Appendix A. Supplementary data

Supplementary data to this article can be found online at https://doi.org/10.1016/j.nicl.2020.102373.

References

Aarnoudse-Moens, C.S., Duivenvoorden, H.J., Weisglas-Kuperus, N., Van Goudoever, J.B., Oosterlaan, J., 2012. The profile of executive function in very preterm children at 4 to 12 years. Dev. Med. Child Neurol. 54 (3), 247–253.
Akazawa, K., Chang, L., Yamakawa, R., Hayama, S., Buchthal, S., Alicata, D., Andres, T., Castillo, D., Oishi, K., Skranes, J., Ernst, T., Oishi, K., 2016. Probabilistic maps of the white matter tracts with known associated functions on the neonatal brain atlas: Application to evaluate longitudinal developmental trajectories in term-born and preterm-born infants. NeuroImage 128, 167–179.
Al-Haddad, C.E., Sebaaly, M.G., Tutunji, R.N., Mehanna, C.J., Saaybi, S.R., Khamis, A.M., Hourani, R.G., 2018. Optic Nerve Measurement on MRI in the Pediatric Population: Normative Values and Correlations. AJNR Am J Neuroradiol 39 (2), 369–374.
Alexander, A.L., Lee, J.E., Lazar, M., Field, A.S., 2007. Diffusion tensor imaging of the brain. Neurotherapeutics 4 (3), 316–329.
Andersson, J.L.R., Jenkinson, M., Smith, S., 2007a. Non-linear registration, aka spatial normalisation. FMRIB Technial Report TR07JA2.
Andersson, J.L.R., Jenkinson, M., Smith, S., 2007b. Non-linear optimisation.
Bach, M., 2007. The Freiburg Visual Acuity Test-Variability unchanged by post-hoc re-analysis. Graefes Arch Clin Exp Ophthalmol 245 (7), 965–971.
Back, S.A., 2017. White matter injury in the preterm infant: pathology and mechanisms. Acta Neuropathol 134 (3), 331–349.
Barb, S.M., Rodriguez-Galindo, C., Wilson, M.W., Phillips, N.S., Zou, P., Scoggins, M.A., Li, Y., Qaddoumi, I., Helton, K.J., Bikhazi, G., Haik, B.G., Ogg, R.J., 2011. Functional Neuroimaging to Characterize Visual System Development in Children with Retinoblastoma. Invest. Ophthalmol. Vis. Sci. 52 (5), 2619.
Bassi, L., Ricci, D., Volzone, A., Allsop, J.M., Srinivasan, L., Pai, A., Ribes, C., Ramenghi, L.A., Mercuri, E., Mosca, F., Edwards, A.D., Cowan, F.M., Rutherford, M.A., Counsell, S.J., 2008. Probabilistic diffusion tractography of the optic radiations and visual function in preterm infants at term equivalent age. Brain 131 (2), 573–582.
Beaudot, W.H.A., 2008. Psykinematix: a new psychophysical tool for investigating visual impairment due to neural dysfunctions. Vision: the Journal of the Vision Society of Japan 21, 19–32.
Beaulieu, C., 2002. The basis of anisotropic water diffusion in the nervous system - a technical review. NMR Biomed. 15 (7-8), 435–455.
Beaulieu, C., Allen, P.S., 1994. Determinants of anisotropic water diffusion in nerves. Magn. Reson. Med. 31 (4), 394–400.
Budny, A., Grochowski, C., 2018. Retinoblastoma. J Educ Heal Sport 8, 204–213.
Chang, L.-C., Jones, D.K., Pierpaoli, C., 2005. RESTORE: Robust estimation of tensors by outlier rejection. Magn. Reson. Med. 53 (5), 1088–1095.
Dubois, J., Benders, M., Cachia, A., Lazeyras, F., Ha-Vinh Leuchter, R., Sizonenko, S.V., Borradori-Tolsa, C., Mangin, J.F., Huppi, P.S., 2008. Mapping the Early Cortical Folding Process in the Preterm Newborn Brain. Cereb. Cortex 18 (6), 1444–1454.
Dubois, J., Dehaene-Lambertz, G., Kulikova, S., Poupon, C., Hüppi, P.S., Hertz-Pannier, L., 2014. The early development of brain white matter: A review of imaging studies in fetuses, newborns and infants. Neuroscience 276, 48–71.
Dunkley, B.T., Vandewouw, M.M., Chakraborty, A., Taylor, M.J., Gallie, B., McCulloch, D. L., et al. 2019. Early life maturation of human visual system white matter is altered by monocular enucleation. Available from: http://dx.doi.org/10.1101/690701.
Ferriero, D.M., Miller, S.P., 2010. Imaging selective vulnerability in the developing nervous system. J. Anat. 217 (4), 429–435.
Fielder, A.R., Moseley, M.J., 2000. Environmental light and the preterm infant. Semin. Perinatol. 24 (4), 291–298.
FitzPatrick, D.R., Heyningen, V.V., 2005. Developmental eye disorders. Curr. Opin. Genet. Dev. 15 (3), 348–353.
Forrester, M.B., Merz, R.D., 2006. Descriptive epidemiology of anophthalmia and microphthalmia, Hawaii, 1986–2001. Birth Defect Res A 76 (3), 187–192.
Fortin, J.-P., Parker, D., Tunç, B., Watanabe, T., Elliott, M.A., Ruparel, K., Roalf, D.R., Satterthwaite, T.D., Gur, R.C., Gur, R.E., Schultz, R.T., Verma, R., Shinohara, R.T., 2017. Harmonization of multi-site diffusion tensor imaging data. NeuroImage 161, 149–170.
Gargallo, P., Oltra, J.S., Yáñez, Y., Segura, V., Balaguer, J., Retinoblastoma, C.A., 2018. Towards an earlier diagnosis. Arch la Soc Española Oftalmol (English Ed) 93, 439–443.
González, E., Steeves, J., Steinbach, M., 2008. Vision with one eye: a review of visual function following unilateral enucleation. Spatial Vis 21 (6), 509–529.
Guo, T., Duerden, E.G., Adams, E., Chau, V., Branson, H.M., Chakravarty, M.M., Poskitt, K.J., Synnes, A., Grunau, R.E., Miller, S.P., 2017. Quantitative assessment of white matter injury in preterm neonates: Association with outcomes. Neurology 88 (7), 614–622.
Halilbasic, M., Jusufovic, V., Musanovic, Z., Cabric, A., 2018. Congenital Bilateral Anophthalmia: a Case Report and Review of Literature. Med Arch 72 (3), 300.
Harsan, L.A., Poulet, P., Guignard, B., Steibel, J., Parizel, N., Loureiro de Sousa, P., Boehm, N., Grucker, D., Ghandour, M.S., 2006. Brain dysmyelination and recovery assessment by noninvasive in vivo diffusion tensor magnetic resonance imaging. J. Neurosci. Res. 83 (3), 392–402.
Hermoye, L., Saint-Martin, C., Cosnard, G., Lee, S.-K., Kim, J., Nassogne, M.-C., Menten, R., Clapuyt, P., Donohue, P.K., Hua, K., Wakana, S., Jiang, H., van Zijl, P.C.M., Mori, S., 2006. Pediatric diffusion tensor imaging: Normal database and observation of the white matter maturation in early childhood. NeuroImage 29 (2), 493–504.
Huang, H., Vasung, L., 2014. Gaining insight of fetal brain development with diffusion MRI and histology. Int. j. dev. neurosci. 32 (1), 11–22.
Jenkinson, M., Bannister, P., Brady, M., Smith, S., 2002. Improved optimisation for the robust and accurate linear registration and motion correction of brain images. Neuroimage 17, 825–841.
Jenkinson, M., Smith, S., 2001. A global optimisation method for robust affine registration of brain images. Med. Image Anal. 5 (2), 143–156.
Johnson, W.E., Li, C., Rabinovic, A., 2007. Adjusting batch effects in microarray expression data using empirical Bayes methods. Biostatistics 8, 118–127.
Källén, B., Robert, E., Harris, J., 1996. The Descriptive Epidemiology of Anophthalmia and Microphthalmia. Int J Epidemiol 25 (5), 1009–1016.
Kasprian, G., Brugger, P.C., Weber, M., Krssák, M., Krampl, E., Herold, C., Prayer, D., 2008. In utero tractography of fetal white matter development. NeuroImage 43 (2), 213–224.
Kelly, C.E., Cheong, J.L., Molloy, C., Anderson, P.J., Lee, K.J., Burnett, A.C., et al., 2014. Neural correlates of impaired vision in adolescents born extremely preterm and/or extremely low birthweight. PLoS One 9, e93188.
Kelly, K.R., DeSimone, K.D., Gallie, B.L., Steeves, J.K.E., 2015. Increased cortical surface area and gyrification following long-term survival from early monocular enucleation. NeuroImage: Clinical 7, 297–305.
Kelly, K.R., McKetton, L., Schneider, K.A., Gallie, B.L., Steeves, J.K.E., 2014. Altered anterior visual system development following early monocular enucleation. NeuroImage: Clinical 4, 72–81.
Kelly, K.R., Zohar, S.R., Gallie, B.L., Steeves, J.K.E., 2013. Impaired Speed Perception but Intact Luminance Contrast Perception in People With One Eye. Invest. Ophthalmol. Vis. Sci. 54 (4), 3058.
Koole, F.D., Velzeboer, C.M.J., Van Der Harten, J.J., 1990. Ocular abnormalities in Patau syndrome (chromosome 13 trisomy syndrome). Ophthalmic Paediatrics and Genetics 11 (1), 15–21.
Kostović, I., Jovanov-Milošević, N., 2006. The development of cerebral connections during the first 20–45 weeks' gestation. Seminars in Fetal and Neonatal Medicine 11 (6), 415–422.
Lebel, C., Gee, M., Camicioli, R., Wieler, M., Martin, W., Beaulieu, C., 2012. Diffusion tensor imaging of white matter tract evolution over the lifespan. NeuroImage 60 (1), 340–352.
Lebel, C., Treit, S., Beaulieu, C., 2019. A review of diffusion MRI of typical white matter development from early childhood to young adulthood. NMR Biomed. 32 (4), e3778.

https://doi.org/10.1002/nbm.v32.410.1002/nbm.3778.
Lecours, AndréRoch, 1989. Paul Ivan Yakovlev and his teachings on cerebral maturation and asymmetries. Journal of Neurolinguistics 4 (2), 273–292.
Lerch, J.P., Sled, J.G., Henkelman, R.M., 2010. MRI Phenotyping of Genetically Altered Mice. Methods Mol Biol 349–361.
McGraw, P., Liang, L., Provenzale, J.M., 2002. Evaluation of Normal Age-Related Changes in Anisotropy During Infancy and Childhood as Shown by Diffusion Tensor Imaging. Am. J. Roentgenol. 179 (6), 1515–1522.
Medixant. RadiAnt DICOM Viewer. 2019. Available from: https://www.radiantviewer.com.
Neveu, M.M., Holder, G.E., Ragge, N.K., Sloper, J.J., Collin, J.R.O., Jeffery, G., 2006. Early midline interactions are important in mouse optic chiasm formation but are not critical in man: a significant distinction between man and mouse. Eur J Neurosci 23, 3034–3042.
O'Connor, A.R., Stephenson, T., Johnson, A., Tobin, M.J., Moseley, M.J., Ratib, S., Ng, Y., Fielder, A.R., 2002. Long-Term Ophthalmic Outcome of Low Birth Weight Children With and Without Retinopathy of Prematurity. Pediatrics 109 (1), 12–18.
Oishi, K., Faria, A.V., Yoshida, S., Chang, L., Mori, S., 2013. Quantitative evaluation of brain development using anatomical MRI and diffusion tensor imaging. Int. j. dev. neurosci. 31 (7), 512–524.
Padilla, N., Alexandrou, G., Blennow, M., Lagercrantz, H., Ådén, U., 2014. Brain growth gains and losses in extremely preterm infants at term. Cereb Cortex 25, 1897–1905.
Pandit, A.S., Robinson, E., Aljabar, P., Ball, G., Gousias, I.S., Wang, Z., et al., 2013. Whole-bain bmapping of structural connectivity in infants reveals altered connection strength associated with growth and preterm birth. Cereb Cortex 24, 2324–2333.
Pavaine, J., Young, J.M., Morgan, B.R., Shroff, M., Raybaud, C., Taylor, M.J., 2016. Diffusion tensor imaging-based assessment of white matter tracts and visual-motor outcomes in very preterm neonates. Neuroradiology 58 (3), 301–310.
Petros, T.J., Rebsam, A., Mason, C.A., 2008. Retinal Axon Growth at the Optic Chiasm: To Cross or Not to Cross. Annu. Rev. Neurosci. 31 (1), 295–315.
Qiu, A., Mori, S., Miller, M.I., 2015. Diffusion Tensor Imaging for Understanding Brain Development in Early Life. Annu. Rev. Psychol. 66 (1), 853–876.
Rakic, P., 1981. Development of visual centers in the primate brain depends on binocular competition before birth. Science 214 (4523), 928–931.
Reed, M.J., Steinbach, M.J., Anstis, S.M., Gallie, B., Smith, D., Kraft, S., 1991. The development of optokinetic nystagmus in strabismic and monocularly enucleated subjects. Behav. Brain Res. 46 (1), 31–42.
Remington, L.A., 2012. In: Clinical Anatomy and Physiology of the Visual System. Elsevier, pp. 1–9. https://doi.org/10.1016/B978-1-4377-1926-0.10001-3.
Rueckert D. Nonrigid registration using free-form deformations: Application to breast MR images. IEEE Trans Med Imaging 1999; 18: 712–721.
Shiell, M.M., 2014. Tonotopic Organization of V5/MT+ in Congenital Anopthalmia: Implications for Auditory Motion Processing and Metamodal Cross-Modal Reorganization. J. Neurosci. 34 (11), 3807–3809.
Smith, S.M., 2002. Fast robust automated brain extraction. Hum. Brain Mapp. 17 (3), 143–155.
Smith, S.M., Jenkinson, M., Johansen-Berg, H., Rueckert, D., Nichols, T.E., Mackay, C.E., Watkins, K.E., Ciccarelli, O., Cader, M.Z., Matthews, P.M., Behrens, T.E.J., 2006. Tract-based spatial statistics: Voxelwise analysis of multi-subject diffusion data. NeuroImage 31 (4), 1487–1505.
Smith, S.M., Jenkinson, M., Woolrich, M.W., Beckmann, C.F., Behrens, T.E.J., Johansen-Berg, H., Bannister, P.R., De Luca, M., Drobnjak, I., Flitney, D.E., Niazy, R.K., Saunders, J., Vickers, J., Zhang, Y., De Stefano, N., Brady, J.M., Matthews, P.M., 2004. Advances in functional and structural MR image analysis and implementation as FSL. NeuroImage 23, S208–S219.
Song, S.-K., Yoshino, J., Le, T.Q., Lin, S.-J., Sun, S.-W., Cross, A.H., Armstrong, R.C., 2005. Demyelination increases radial diffusivity in corpus callosum of mouse brain. NeuroImage 26 (1), 132–140.
Sullivan, E.V., Zahr, N.M., Rohlfing, T., Pfefferbaum, A., 2010. Fiber tracking functionally distinct components of the internal capsule. Neuropsychologia 48 (14), 4155–4163.
Sun, S.-W., Liang, H.-F., Trinkaus, K., Cross, A.H., Armstrong, R.C., Song, S.-K., 2006. Noninvasive detection of cuprizone induced axonal damage and demyelination in the mouse corpus callosum. Magn. Reson. Med. 55 (2), 302–308.
Suzuki, Y., Matsuzawa, H., Kwee, I.L., Nakada, T., 2003. Absolute eigenvalue diffusion tensor analysis for human brain maturation. NMR Biomed. 16 (5), 257–260.
Tyszka, J.M., Readhead, C., Bearer, E.L., Pautler, R.G., Jacobs, R.E., 2006. Statistical diffusion tensor histology reveals regional dysmyelination effects in the shiverer mouse mutant. NeuroImage 29 (4), 1058–1065.
Verma, A.S., FitzPatrick, D.R., 2007. Anophthalmia and microphthalmia. Orphanet J Rare Dis 2 (1). https://doi.org/10.1186/1750-1172-2-47.
Volpe, J.J., 2009. Brain injury in premature infants: a complex amalgam of destructive and developmental disturbances. The Lancet Neurology 8 (1), 110–124.
Wong, N.A., Rafique, S.A., Kelly, K.R., Moro, S.S., Gallie, B.L., Steeves, J.K.E., 2018. Altered white matter structure in the visual system following early monocular enucleation: Altered White Matter After Early Enucleation. Hum. Brain Mapp. 39 (1), 133–144.
Yakovlev, P.I., Lecours, A-R. 1967. The myelogenetic cycles of regional maturation of the brain. In: Regional Development of Brain in Early Life. p. 3–70.
Young, J.M., Morgan, B.R., Whyte, H.E.A., Lee, W., Smith, M.L., Raybaud, C., et al., 2017. Longitudinal study of white matter development and outcomes in children born very preterm. Cereb Cortex 27 (8), 4094–4105.
Young, J.M., Vandewouw, M.M., Mossad, S.I., Morgan, B.R., Lee, W., Smith, M.L., Sled, J.G., Taylor, M.J., 2019. White matter microstructural differences identified using multi-shell diffusion imaging in six-year-old children born very preterm. NeuroImage: Clinical 23, 101855. https://doi.org/10.1016/j.nicl.2019.101855.